ADDIS ABABA UNIVERSITY

SCHOOL OF INDUSTRIAL AND MECHANICAL ENGINEERING

MASTER'S DEGREE THESIS

SIMULATION OF RAIL VEHICLE FLEXIBLE WHEEL SET ON CURVE NEGOTIATION

BY MAEDOT MENBERU

APRIL, 2017

ADDIS ABABA, ETHIOPIA

Acknowledgement

I would like to express my sincere gratitude to my advisor Mr. Habtamu Tekubet (AAU,SMIE instructor and railway engineering graduate studies coordinator of Addis Ababa university)for his kindness, encouragement, support and fruitful advises and follow up throughout the preparation of this thesis.

I would like to express my truthful gratitude to Ethiopian Railway Corporation for giving me a chance to study master's degree in the field of railway vehicle engineering and to AAU,SMIE instructors who taught me valuable topics of railway engineering courses which made me to be more interested for this master's program and the profession.

Finally I wish to express my deepest gratitude to all who assist me in different ways in my study time.

Abstract

Railway vehicle wheelsets suffer a great many dynamic load cycles as they rotate and excessive contact force happen on wheelset during a rail vehicle curve negotiating which makes wheelsets the most critical stressed part of a railway rolling stock and they are likely prone to a wide variety of dynamical phenomena such as static and dynamic instabilities, lateral guidance problems on curved track and ride quality. Mostly multibody models used by railway vehicle designers use totally rigid wheelsets without considering flexibility, thus leading to possible result errors vehicle under study compared with actual. The introduction of the wheelset structural flexibility allows for the determination of different quantities such as strains and stresses, and in some cases it is used to avoid numerical problems in the simulations due to a rigid connection between the axle and the wheels.

This thesis considers the development of flexible wheelset model on curves through numerical simulations so that to study the influence wheelset flexibility on dynamic behaviors of wheel rail contact. Development of flexible wheelset model simulation is done by using the method called FEMBS, is an interface program between finite element (FE) analysis codes and SIMPACK. FEMBS generates input data for flexible bodies which are used for multibody system (MBS) simulations. The flexible wheelset model was developed by FEM software ANSYS that calculates a wheel deflection. Subsequently, a stress distribution with corresponding frequencies at contact patches for driving wheel is formulated. Then the ANSYS model is imported in to a multibody simulation software SIMPACK. For a simulation output results comparisons purpose a rigid wheelset the model is also simulated on SIMPACK parallely. And small radius curve exposed to severe corrugation growth on the metro of Addis Ababa light rail transit (AALRT) was selected as reference.

The simulation results indicates on mid simulation time lateral force of flexible and rigid wheelsets are 100KN and 93KN respectively. The angle of attack at wheel/rail interface of the simulation result after about 2.5 second of flexible wheelset is greater than in average of the rigid wheelset model. And the wear result shows that the flexible wheelset wear no. is larger average than the rigid wheelset. Thus this study reveals that the flexibility importance of pertinent wheelset model for simulating and investigating different aspects of the vehicle-track dynamic interaction.

List of figure

Glossary of Nomenclature

V	The load (vertical force) on the wheel
L	The load (lateral force) on the inner wheel
b	Half the gauge
y	Lateral displacement of the wheelset
$2l$	Track gauge
R	The radius of the track curve
r_o	The radius when the wheelset is central
r_{inner}	Inner radius of wheel
r_{outer}	Outer radius of wheel
h	A height between rail car c.g and top of rails
$F_{inertia}$	Inertia load
τ_{weight}	Torque due to the weight
V_{max}	Vehicle maximum speed
S	Rail superelevation height
θ	Rail cant angle
λ	Conicity of wheel tread / inclination
δ	Wheel flange angle
E	Combined Young's modulus
ν	Poisson ratio
μ	Friction coefficient
α	Attack angle

Contents

1. INTRODUCTION

1.1Background

In our country Ethiopia AALRT is the tram transportation recently on operation. These trams are constructed along the East-west and South-north lines in Addis Ababa, total length of main lines is around 31.025km, where the East-west main line is around 16.998km long; the South-north main line is around 16.689km long. Both lines share the same section of around 2.662km in the urban areas. The vehicles are operating under the ground, on the ground, along curves and on elevated lines. It is ensured that the vehicles be able to safely operate at lower speeds with Grade 8 wind (20.7m/s) when operating on the ground and elevated lines and that the empty vehicles be able to safely park on the lines with Grade 9 wind (24.4m/s). The vehicles shall be maintained and checked inside the on-ground depot and parked outside the depot. The vehicles shall be shipped by sea and transported by road to the depots. The vehicles shall be manually operated and returned back. The local natural environment conditions of the manufacturer of the vehicles shall be considered .Even though there is a need for new train conception and optimizing existing designs locally in the future as trains are running faster and the freight loads are becoming heavier [21].

Dynamics of railway vehicle and vehicle-track interaction covers a wide range of technical subjects such as vehicle oscillations and stability, track forces between wheel and rail, derailment due to vehicle oscillations and track forces, derailment due to lose of lateral constraint at wheel and rail interface arising from operating speed, wear of wheel and rails due to vehicle oscillations and track forces, passenger comfort and loads displacements, sudden safety risks due to track faults, fatigue of track and vehicle components, air borne and structure borne sound propagation to the vehicle and surrounding environment [18].External inputs such as rail irregularities, sudden disturbances like sharp curve, switch, breaking or accelerating and other failures, all affect the dynamic behavior of a railway vehicle. This problem can be studied by dynamic response analysis of rail vehicle. Problems take place due to these unwanted inputs while railway vehicle begin to move indifferent directions as pitch, vertical, roll, yaw and lateral directions. These movements cause vibrations and damage in railway components with uncomfortable ride passenger. Lateral displacements happen due to defects and irregularities in the track which cause different undesirable motions like roll, yaw, and pitch. Lateral forces occur in the wheel-rail

contact patch plane owing to interactions between the wheel and the rail which force wheelsets to move laterally and may climb the rail [8].

Generally, empirical engineering development was able to keep abreast of the requirements of ride quality and safety. Then, increasing speeds of trains and the greater potential risks arising from instability stimulated amore scientific approach to vehicle dynamics. Realistic calculations, supported by experiment, on which design decisions based, were achieved in the past years and as the power of the digital computer increased so did the scope of engineering calculations, leading to today's powerful modeling tools.

1.2 Review of literatures

The influence of the wheelset bending, torsional and umbrella modes on the lateral vehicle stability was examined by Kaiser and Popp (August 2004), comparing the running behavior of rigid respectively flexible wheelsets. The authors mentioned that the strongest influence on the running behavior is caused by the wheelset flexural displacements. The out-of-plane bending causes a deflection of the wheelset in vertical and lateral directions and leads to additional creepage.

Andersson C and Abrahamsson T (2000) studied the influence of wheelset flexibility on longitudinal and normal track forces was investigated through numerical simulations involving a wheelset with rigid or flexible wheelset axle. The wheelset first torsional mode was excited by means of a sinusoidal corrugation on both rails with a corresponding wavelength of 0.66 m, the corrugation being out-of-phase by 180 degrees. Hence, for a running speed of 160 km/h (44.4 m/s) the excitation frequency around 67 Hz corresponds to the wheelset fundamental torsion mode. The authors stated that a flexible wheelset axle results in lower longitudinal force as compared to the rigid case and reported a rather small influence of the wheelset flexibility on the normal contact force.

Wheel-out of roundness (OOR) or polygonization is an imperfection on the wheel tread that can lead to detrimental influence on both tracks and wheels, result in high impact loads and cause an increase in rolling noise. The classification of wheel imperfections and their influence on the vehicle-track dynamics were reviewed in Johansson A and Nielsen J (1998) also surveyed the possible causes of the formation and development of wheel OOR which include, among other, the influence of wheelset structural flexibility. The enlargement of wheelset OOR was also investigated by Morys B (1999).The author stated that the normal force accelerates the wheel vertically causing

a bending oscillation of the wheelset which in turn leads to lateral slip and material excavation. The material excavation due to longitudinal slip and spin plays a minor role in the OOR growth.

Matsumoto et al. (1996) studied the mechanism of rail corrugation formation on curved track. The authors indicated that the axle over loading s has an influence on the rail head wear index. The larger the axle overloading, the larger the wear index is. However, the axle torsional stiffness does not influence the wavelength of corrugation which is mainly influenced by the vertical system dynamics rather than by the axle torsional oscillation.

A linear wheel-track model aiming at investigating the rail corrugation at narrow curves for ballasted and slab tracks was developed by Tassilly and Vincent (1991). According to the authors the corrugation formation on the leading axle on a ballasted track is significant in the frequency range of 60-80 Hz, at proximity of the wheelset first bending mode, where a slight fluctuation in the vertical force can cause large transverse sliding. For the trailing axle, a longitudinal wear function is highest at around 55 Hz, which can be related to the wheelset first, highly undamped, torsion mode. This phenomenon is more likely to occur on narrow curves rather than on a straight track. Similar findings and conclusions were drawn by Meinders and Hempelmann et al (September 1992). The latter indicated that the primary influence of the wheelset flexibility on formation of corrugation is caused by the coupling of its vertical and lateral dynamics through axle bending.

As can be seen, the majority of the articles study the influence of wheelset flexibility on contact forces and the development of wear patterns on the wheels and tracks at low-frequency. Despite the wheelset model should be analyzed on a curve where a very large number of vibration modes (at high frequency) in order to achieve a suitable representation of real systems.

1.3 Problem Statement

Railway vehicle wheelsets suffer a great many dynamic load cycles as they rotate and they are likely prone to a wide variety of dynamical phenomena such as static and dynamic instabilities, lateral guidance problems on curved track and ride quality. External inputs such as rail irregularities, sudden disturbances like sharp curve negotiation affect the dynamic behavior of a railway vehicle. For all that, up to now only few realistic data are available about the wheel/rail forces acting within narrow curves.

Mostly multibody models used by railway vehicle designers use totally rigid wheelsets without considering flexibility, thus leading to possible result errors vehicle under study compared with

actual. Structurally wheelset axle deflects and makes wheels to be deformed. This phenomenon causes fluctuations in the wheel-rail contact that contributes to the additional development of undesirable wheel-rail contact behaviors and hence it needs a detail study.

1.4 Objective

The main objective of this study is simulating flexible rail vehicle wheelset using FEMBS (an interface program between finite element (FE) analysis codes and SIMPACK), so that identifying the effect wheelset flexibility on dynamic contact behavior on a curve. And the specific objectives are:

- Developing flexible wheelset model simulation using FEMBS(an interface program between finite element analysis of ANSYS codes and multi body simulation software SIMPACK)
- Modeling and simulating a rigid wheelset using SIMPACK for result comparisons purpose.
- Comparing simulation response results of flexible and rigid wheelset models and studying the influence of wheelset flexibility on running behavior.

1.5 Methodology

In this thesis development of flexible wheelset model simulation is done by using the method called FEMBS, is an interface program between finite element (FE) analysis codes and SIMPACK. FEMBS generates input data for flexible bodies which are used for multibody system (MBS) simulations. The flexible wheelset model was developed by FEM software ANSYS that calculates a wheel deflection. Subsequently, a stress distribution with corresponding frequencies at contact patches for driving wheel is formulated. Then the ANSYS model is imported in to a multibody simulation software SIMPACK. For a reference purpose a rigid wheelset the model is also simulated by SIMPACK parallely. A small radius curve exposed to severe corrugation growth on the metro of Addis Ababa light rail transit (AALRT) was selected as reference.

1.6 Scope & Limitations

This thesis provides the following scopes.

- A literature review on methods used in measuring and modelling the wheelset structural flexibility is provided. Also, the influence of these flexibilities on the overall vehicle-track dynamic interaction is included.
- Identification of models of railway track dynamic behavior that are suitable to examine influence of wheelset flexibility.
- Simulation of two different wheelsets of rigid and flexible so that to identify dynamic properties wheel and rail contacts.

And it is limited to:

- This thesis will not develop a model to study track flexibility on the vehicle-track dynamic interaction.
- It includes no practical benchmark or other simulation model; rather wheelset dynamic analysis responses using multibody simulation results will be interpreted.

2. THEORETICAL AND ANALYTICAL FOUNDATION OF RAIL VEHICLE WHEELSET

This chapter is intended to describe basic principles which are relevant to the point of discussion to carry out the study.

2.1 Rail vehicle wheel set construction

A wheel set comprises two wheels rigidly connected by a common axle. Wheel set is supported on bearings mounted on the axle journals.

Railway wheelsets carry out a surprisingly wide range of functions:

- They carry load
- They offer a low resistance to motion
- It is means of delivering traction and braking forces
- Offer necessary distance between vehicle and track
- It guides that determine motion within rail gauge, including curves and switches.
- They offer a return path for electric traction current and they provide a key element in the train detection process essential to the signaling system.
- It is transmitting traction and braking forces to the rails to accelerate and decelerate the vehicle.

A conventional wheelset consists of two conical wheels rigidly connected to a common wheelset axle, axle-boxes mounted on the two axle ends through roller bearings, and often axle-mounted or wheel-mounted brake discs. The wheelset forms an important entity of a railway vehicle. It helps carrying the vehicle through the primary suspension, supports the vehicle at rolling, guides the vehicle, transfers the longitudinal forces at braking and in case of a powered wheelset, at traction. [26].

The design of the wheel set depends on:

- The type of the vehicle (traction or trailing),
- The type of braking system used (shoe brake, brake disc on the axle, or brake disc on the wheel)
- The construction of the wheel center and the position of bearings on the axle (inside or outside)
- The desire to limit higher frequency forces by using resilient elements between the wheel centre and the tyre.

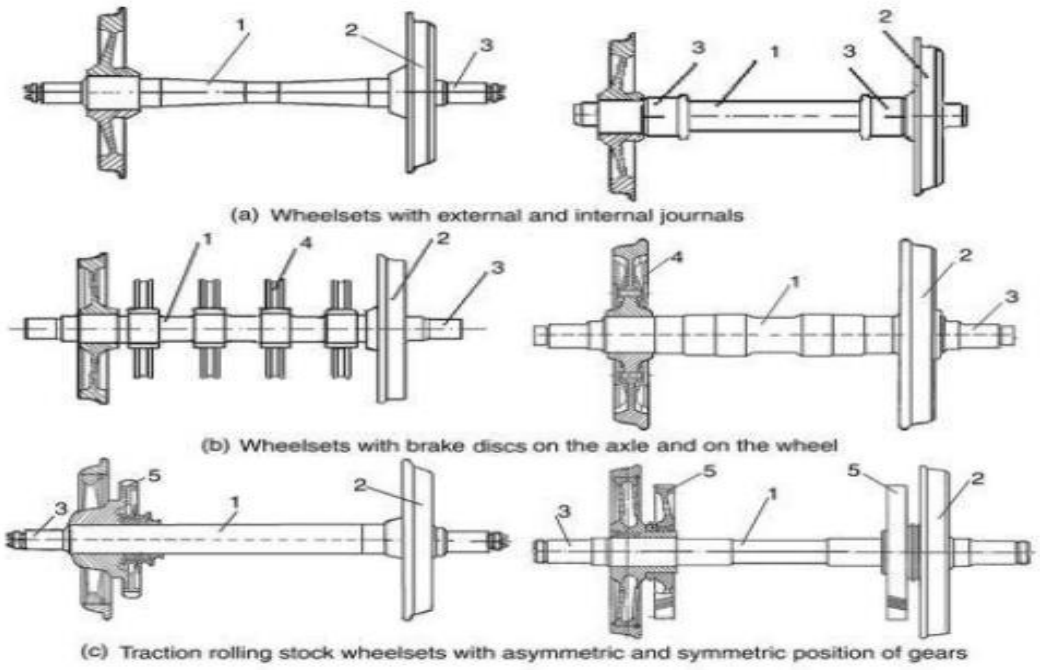

Figure *2.1Main type of wheel set design: (a) with external and internal journals; (b) with brake discs on the axle and on the wheel; (c) with asymmetric and symmetric position of gears (1,axle; 2, wheel; 3, journal; 4, brake disc; 5, tooth gear) [26].*

Basic requirements of wheelset:

- ☞ Enough strength to maintain safety and fatigue life
- ☞ Light weight to reduce w/r interaction forces
- ☞ Low traction resistance and low wear
- ☞ Suitable for straight operation and curving

- ☞ Good derailment prevention

2.2Wheel-rail interaction

Wheel-rail interface distinguishes railways from other forms of land transports. In order to simulate the wheel-rail interaction force, the contact between the wheel and rail must be established by a well-defined method, since an accurate solution of the rolling contact problem is quite complex. The essential characteristic of the wheel-rail contact is its extreme stiffness in vertical direction. The area of contact is generally very small, while the interface supports the traction, braking, and curving forces apart from the vertical forces. The interaction between the vehicle and the track system is achieved at the wheel/rail interfaces through wheel/rail force compatibility [15].

The wheel set rests on two rails fixed to the sleepers. A typical wheelset on rails is shown in figure 2.2. Wheelset runs on rails normally inclined (canted) at 1 in 40 (1 in 20). The gap between the flange of the wheel and the gauge side of the rail such that it allows 4-7mm lateral wheelset displacement before flange contact occurs [12].

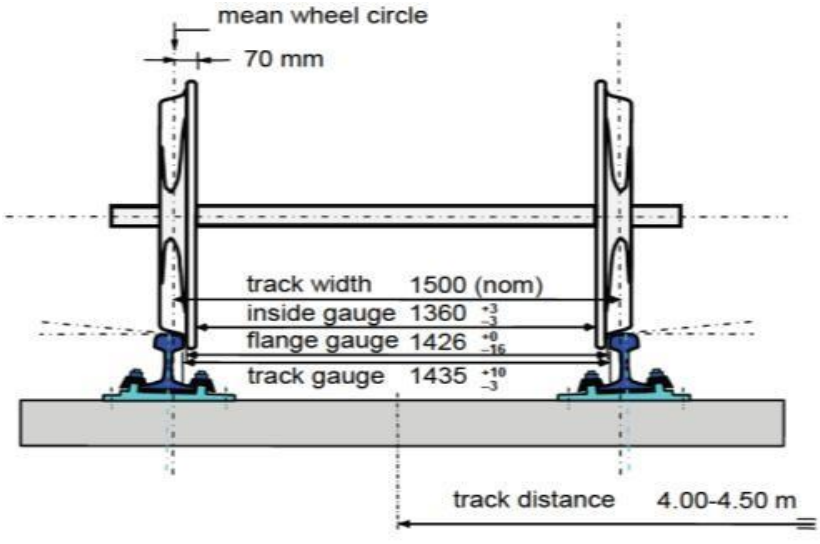

Figure 2.2 *Wheelset - track system*

The shapes of wheel/rail surfaces (tread, flange root flange and flange of the wheel, rail head, gauge corner, and gauge face of the rail are significant to vehicle stability, wheel/rail interaction forces, contact stresses, and wear characteristics.

Vehicle and track dynamics systems interact via wheel/rail interface, using output from one model as input for another, and vice-versa. For example, track irregularities can be used as an input for wheel/rail contact, causing disturbances in contact forces, which in turn will be used as an input for the vehicle model. To determine forces in wheel/rail contact, values of creepage and spin are required, which can be obtained from analysis of geometric contact between wheelset and track [9].

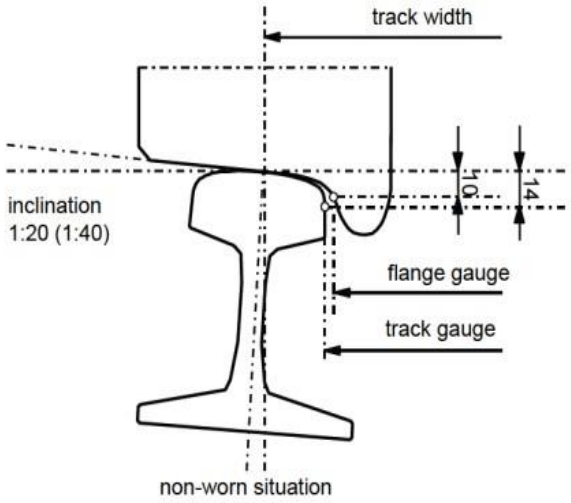

Figure 2.*3 Track and flange gauge*

Wheels and axles are the most critical parts of the railway rolling stock. Mechanical failure or error on design dimensions can cause derailment. Simple linear models of vehicles with wheelsets represented by double cones on specific tracks or circular profiles determine that the most unstable modes of vibration are vehicle hunting modes, whether on the car body, bogie or wheelset. Running under unstable conditions leads to increased lateral displacement of the wheelsets which causes impact between the wheel flanges and tracks. When including flexibility of the wheelsets in the dynamic simulation model, it must represent adequately the displacement and internal rotation of the wheel affecting the creepages in the wheel/rail contact, which are:

- Longitudinal and lateral displacement
- Roll, torsion and yaw

The example shown here uses a right-curving section of track [16]. The focus is on the left-side wheel, which is more involved with the forces critical to guiding the railcar through the curve.

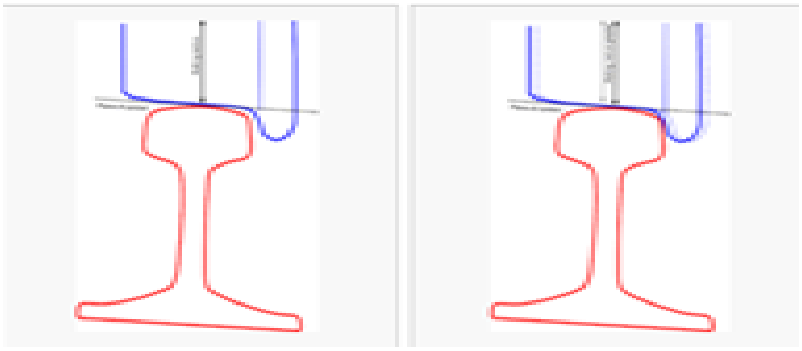

Diagram 2.1 *Diagram 2.2*

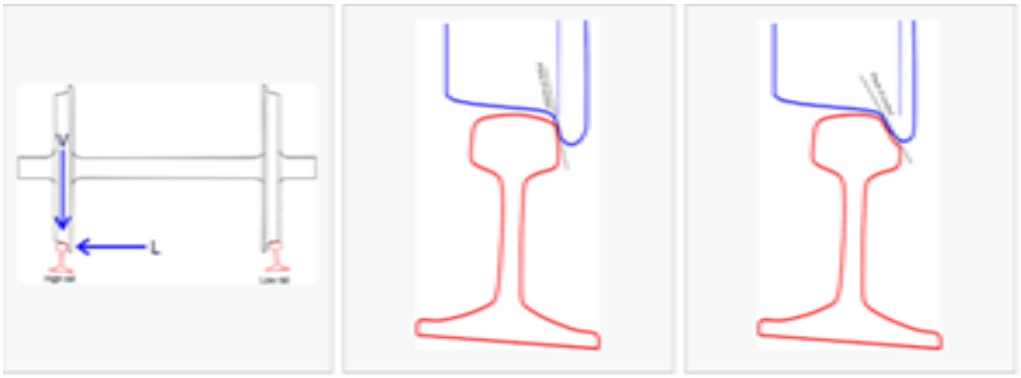

Diagram 2.3 *Diagram 2.4* *Diagram 2.5*

Figure 2.4 Wheel and rail diagrams at right-curving section of track

Diagram 2.1shows the wheel and rail with the wheelset running straight and central on the track. The wheelset is running away from the observer. (Note that the rail is shown inclined inwards; this is done on modern track to match the rail head profile to the wheel tread profile.)

Diagram 2.2 shows the wheelset displaced to the left, due to curvature of the track or a geometrical irregularity. The left wheel (shown here) is now running on a slightly larger diameter; the right wheel opposite has moved to the left as well, towards the center of the track, and is running on a slightly smaller diameter. As the two wheels rotate at the same rate, the forward speed of the left wheel is a little faster than the forward speed of the right wheel. This causes the wheelset to curve to the right, correcting the displacement. This takes place without flange contact; the wheelsets steer themselves on moderate curves without any flange contact. The sharper the curve,

the greater lateral displacement necessary to negotiate it. On a very sharp curve (typically less than about 500 m or 1,500 feet radius) the width of the wheel tread is not enough to achieve the necessary steering effect, and the wheel flange contacts the face of the high rail.

Diagram 2.3 shows the two forces L and V are shown. The load (vertical force) on the outer wheel is designated V. Sliding requires a considerable force to make it happen, and the friction force resisting the sliding is designated "L", the lateral force. The wheelset applies a force L outwards to the rails, and the rails apply a force L inwards to the wheels. Note that this is quite independent of "centrifugal force". However at higher speeds the centrifugal force is added to the friction force to make L. The steel-to-steel contact has a coefficient of friction that may be as high as 0.5 in dry conditions, so that the lateral force may be up to 0.5 of the vertical wheel load.

Diagram 2.4 shows flange contact, the wheel on the high rail is experiencing the lateral force L, towards the outside of the curve. As wheel rotates, flange tends to climb up the flange angle. It is held down by the vertical load on the wheel V, so that if L/V exceeds the trigonometrical tangent of t flange contact angle, climbing will take place. The wheel flange will climb to the rail head where there is no lateral resistance in rolling movement, and a flange climbing derailment usually takes place. The flange contact angle is quite steep, and flange climbing is unlikely.

However if rail head is side-worn (side-cut) or the flange is worn, as shown in **Diagram 2.5** the contact angle is much flatter and flange climbing is more likely. Once the wheel flange has completely climbed on to the rail head, there is no lateral restraint, and the wheelset is likely to follow the yaw angle, resulting in t wheel dropping outside rail. An L/V ratio or derailment coefficient greater than 0.6 is considered to be hazardous.

2.3 WHEELSET CURVE NEGOTIATION PERFORMANCE MEASURES

During curving of railway vehicles, normal and tangential forces and relative sliding are created in the contacts between wheel and rail. Due to the associated damage in the forms of wear and rolling contact fatigue, the predicted life of curved track is less than half of that for tangent track.

Optimal curve negotiation or perfect steering is achieved when each wheelset in a vehicle adopts a radial position and displaces laterally so that it rolls without slip around the curve. As such, the wheelset lateral excursion from the track center line and the wheelset angle of attack with respect to radial alignment are natural performance indices. An undesirable situation exists when this

indices reach large magnitudes. The derailing tendency of a vehicle are associated with the ratio of lateral flange force to vertical wheel load. When this ratio exceeds a critical value, there exists a situation conducive to a flange climbing type occur. [13].

On a gentle curve, coned wheels maintain pure rolling motion by moving laterally outward and adopting a radial position. In this way, the wheel on the outside of the curve runs on a larger radius (and therefore circumference) and can travel the greater distance at common angular speed; whereas the wheel on the inside of the curve rolls on its smaller radius and travels the smaller distance. So a wheelset with coned wheels maintains pure rolling motion in a gentle curve, without flange contact, if it moves laterally outward a distance *y* from the center of the track and adopts a radial position as shown on figure below.

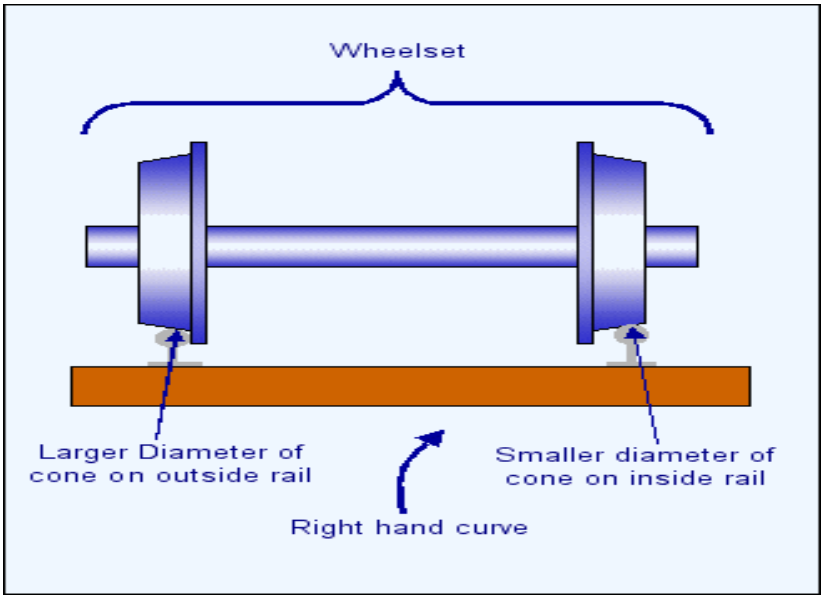

Figure 2.5 The location of the wheels in relation to the rails on curved track.

Flanges are a necessary precaution but they ought never to touch rail and therefore they cannot be said to keep the wheels on the rails. They ought not to come into action except to meet an accidental, lateral force. The wheels are made conical, the smaller circumference at the outer edge. If anything throws the wheels in the slightest degree to one side the wheel is immediately rolling on a larger circumference than the other and the tendency to roll back is introduced. The carriage is kept always in the middle of the track.

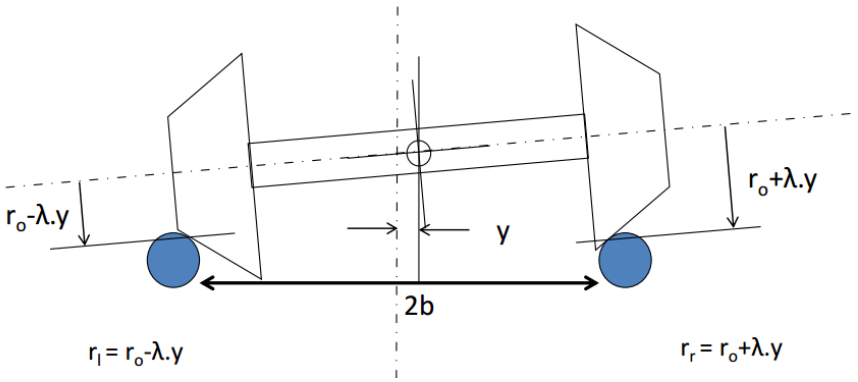

Figure *2.6 Motion of a free wheelset with the necessary dimensions*

2.3.1Radius of Curvature

Radius of railroad curves affects construction costs and operating costs of railroad track, and in combination with super elevation and other track geometry, determines the maximum safe speed of a curve. A major factor that comes into play is minimum track curve radius. Minimum curve radii for railroads are designed to allow a certain operating speed and are constrained by the mechanical ability of the rolling stock to adjust to the curvature. It is possible to design tracks with relatively short radii. However, extremely curves are generally undesirable. In addition, the universe of available rolling stock becomes larger as the minimum curve radius increases. For passenger trains that must keep commuters to strict timetables, operating speeds are often much higher than those for freight traffic. Therefore curves on dedicated passenger lines are ideally much gentler, with minimum radii [23].

2.3.2 Lateral displacement

Perfect curving is a free wheelset motion that happens while the train is travelling along a track path with no or minimum lateral instability.

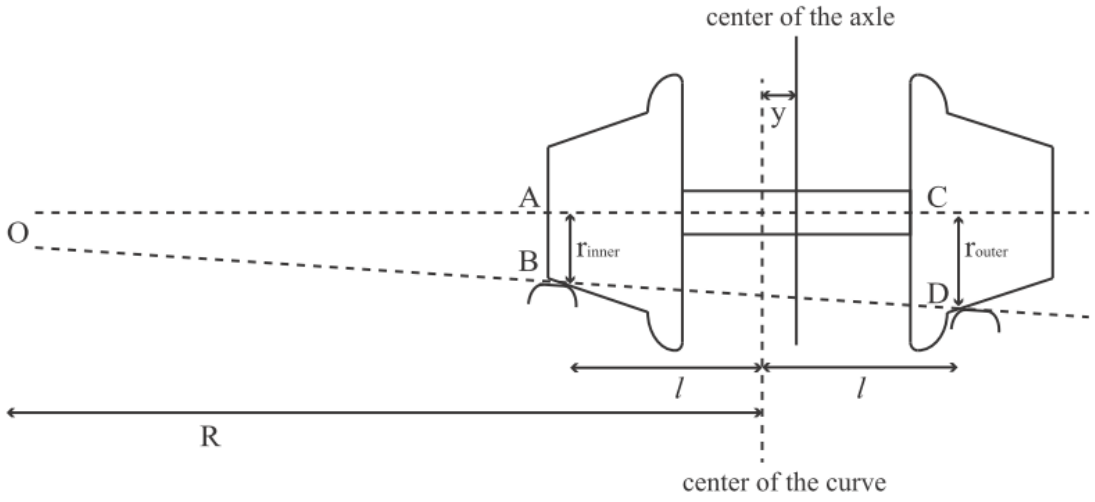

Figure 2.*7 Wheelset lateral displacement*

Using properties of similar triangles an equation for perfect curving can be derived from figure 2.5,

$$\frac{r_{inner}}{R-l}=\frac{r_{outer}}{R+l} \qquad (2.1)$$

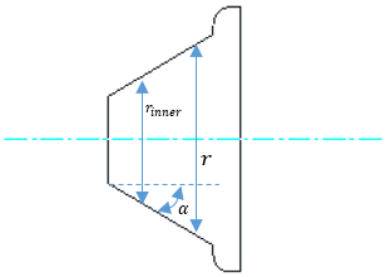

Figure 2.8Wheel profile diagram

where *R* is the radius of curve, 2*l* is the track width or gauge (the lateral distance between the points of contact of the wheels with the rails), r_{inner} is the radius of the wheel on the inside of the curve at the point of contact with the rail and r_{outer} is similarly the radius of the wheel on the outside of the curve at the point of contact with the rail. Defining the normal running radius, *r* to be the radius of both wheels when the wheelset is centered on the track, then it can be rewritten as r_{inner} and r_{outer} in terms of the conicity of the wheelset, λ, and the lateral displacement of the wheelset, *y*.

$$r_{inner}= r - \lambda y \qquad (2.2)$$

$$r_{outer} = r + \lambda y \tag{2.3}$$

By substituting these expressions for r_{inner} and r_{outer} into the similar triangles relation, we can solve for the lateral displacement y in terms of physical parameters of the wheel rail system: the tread conicity, α, normal wheel radius r, track gauge, $2l$, and radius of curvature, R:

$$\frac{r-\lambda y}{R-l} = \frac{r+\lambda y}{R+l} \tag{2.4}$$

$$(R-l)(r+\lambda y) = (r-\lambda y)(R+l)$$

$$rl - \alpha yR = -rl + \alpha yR$$

$$2rl = 2\lambda yR$$

$$y = \frac{rl}{R\lambda} \tag{2.5}$$

2.3.3Maximum speed

- **Maximum Operating Speed along curve On a Flat Curve**

On a flat curve centrifugal inertial loading is trying to tip the locomotive clockwise about the pivot point (the bottom of the right wheel). This rotation is resisted by the weight of the locomotive (also acting through its center of gravity), which tries to rotate locomotive counterclockwise [22].

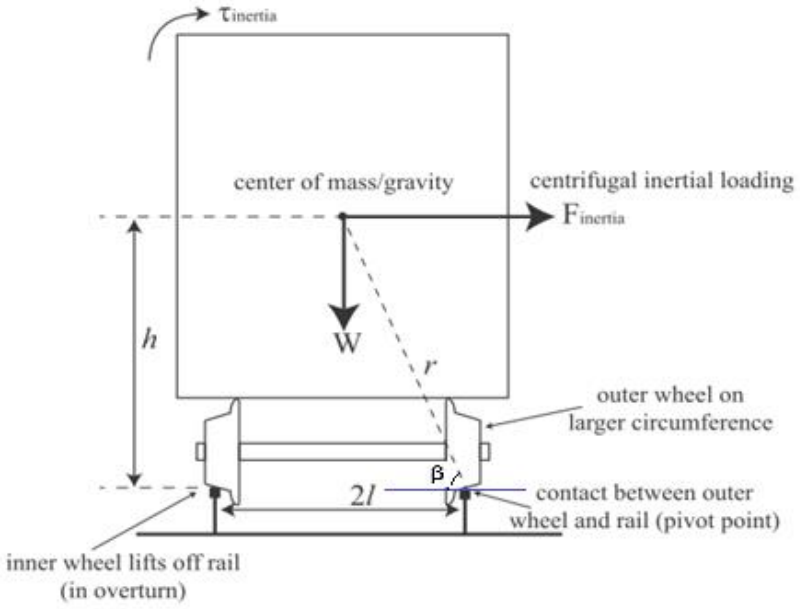

Figure 2.9 Railcar force diagram on a flat curve

Locomotive's weight and inertial load both exert a torque. The inertial load tries to rotate the locomotive with a clockwise torque equal to $\tau_{inertia} = F_{inertia} \times r$, where r is vector pointing from center of mass to the pivot point. For a railcar with center of mass at a height h above the top of the rails and located at center of the gauge (a horizontal distance l from either rail), the vector cross product is equal to:

$$\tau_{inertia} = F_{inertia} \sin(\beta) = \left(\frac{W}{g}\right)\left(V^2 \frac{1}{R}\right) h \qquad (2.6)$$

The torque from the locomotive's weight, transferred between outside wheel and rail via adhesion, tries to resist overturning torque from centrifugal inertial loading. The torque from the locomotive's weight is given by

$$\tau_{weight} = Wr(\sin(90° - \beta) = Wl \qquad (2.7)$$

Tipping will occur when the torque from inertial load is slightly larger than the torque from the locomotive's weight resisting overturning torque. Since centrifugal inertial loading depends on the speed of the locomotive, there is a critical speed at which, all geometries of the curve held constant, the overturning and resisting torques are equal. So setting $\tau_{inertia} = \tau_{weight}$ we can solve for this critical speed [22],

$$\left(\frac{W}{g}\right)\left(V^2\frac{1}{R}\right)h = Wl$$

$$\left(V^2\frac{1}{R}\right) = \frac{lg}{h}$$

$$V_{max} = \sqrt{\frac{lgR}{h}} \qquad (2.8)$$

- **On a Superelevated Curve**

In modern industrial practice, many tracks are designed so that rails are not flat on curves. Instead, the curve is banked so that the outside rail on a curve is elevated higher than the inside rail. This superelevation (or cross level in the US) is usually characterized by the height difference between the tops of the rails, but can also be measured in terms of angle or cant. The relationship between the cant angle and superelevation height is dictated by the rail gauge according to simple right-triangle geometry [22]:

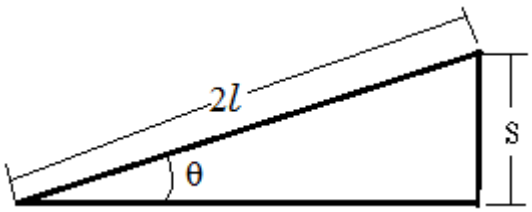

Figure 2.10 cant angle and superelevation height is dictated by the rail gauge

$$\sin\theta = \frac{s}{2l} \qquad (2.9)$$

A raised outside rail rotates the train toward the inside of the curve and helps fight off overturning rotation toward the outside of the curve caused by the centrifugal inertial loading. Since some of inertial torque is counteracted by the weight, the railcar can traverse the curve at a higher speed before overturning. In addition to allowing trains to travel through turns at higher maximum speeds, superelevation also helps keep the wheel flanges from pressing the rails, minimizing friction and wear.

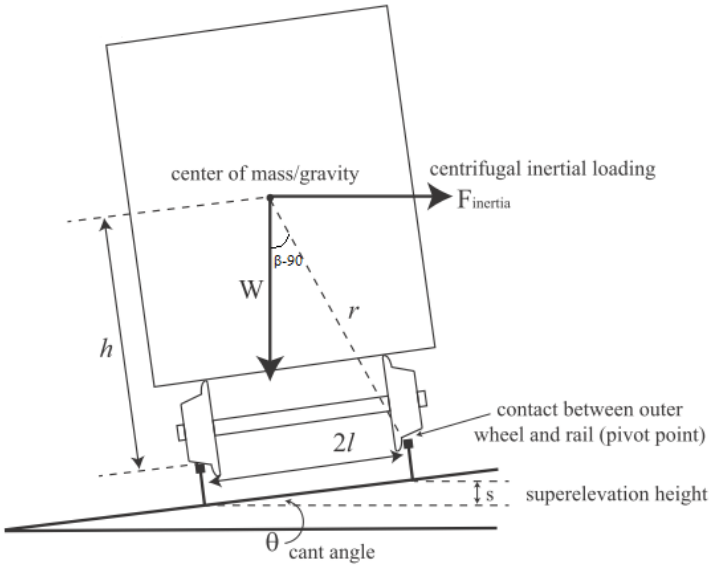

Figure 2.11 Railcar force diagram on a superelevated curve.

With a superelevated track torque due to inertial loading still acts around the pivot of the contact point between the outside wheel and the rail. However, angle between the inertial loading force and pivot vector, *r*, has been effectively reduced by the superelevation angle or cant angle, θ, as the car tilts in relation to the center of the curve.

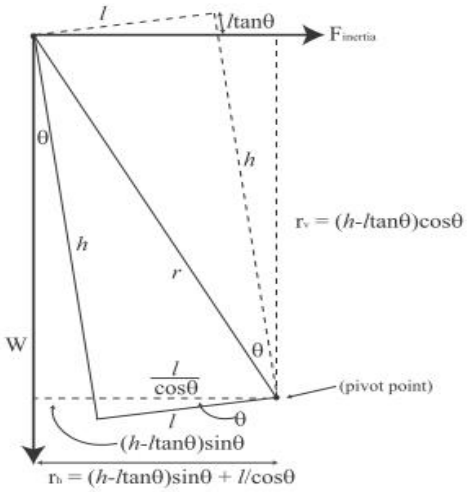

Figure2.12 Geometry of the forces and torque arm for a railcar on a slightly superelevated curve

Given the geometry between the forces on the railcar and the torque arm from the center of the railcar mass to the outside wheel contact point (see Figure), we can find that the vertical distance between the pivot point and the inertial loading force is $r_v = (h - l \tan\theta)\cos\theta$. So torque from inertial loading is given by the expression:

$$\tau_{inertia} = F_{inertia} x r_v \tag{2.10}$$

$$= F_{inertia}[(h - l\tan\theta)\cos\theta]$$

$$= F_{inertia}[h\cos\theta - l\sin\theta]$$

$$\tau_{inertia} = \left(\frac{W}{g}\right)\left(V^2\frac{1}{R}\right)[h\cos\theta - l\sin\theta] \tag{2.11}$$

Similarly, we can find the horizontal distance between pivot point and weight force vector in terms of l, h, and θ: $r_h = (h - ltan\theta)sin\theta + \frac{1}{cos\theta}$

With this we find that the torque due to the weight on a superelevated curve, $\tau_{weight} = W \times r$ is given by:

$$\tau_{weight} = W\left[(h - l\tan\theta)\sin\theta + \frac{l}{\cos\theta}\right]$$

$$= W\left[h\sin\theta - \frac{l}{\cos\theta}(-\cos^2\theta)\right]$$

$$\tau_{weight} = W[h\sin\theta + l\cos\theta] \tag{2.12}$$

Just as in the flat curve situation, the maximum or critical speed is where the torque toward the inside of curve from the weight exactly counteracts the torque toward the outside of the curve from the inertial loading. So to find an expression for the maximum speed, we set $\tau_{inertia}$ equal to τ_{weight}:

$$\left(\frac{W}{g}\right)\left(V^2\frac{1}{R}\right)[h\cos\theta - l\sin\theta] = W[h\sin\theta + l\cos\theta = \left(V^2\frac{1}{Rg}\right) = \frac{h\sin\theta + l\cos\theta}{h\cos\theta - l\sin\theta}$$

$$V_{max} = \sqrt{\frac{Rg[h\sin\theta + l\cos\theta]}{hcos\theta - l\sin\theta}} \tag{2.13}$$

2.3.4 Wheel -track forces

Vehicles shall be able to run over the normal range of vertical track irregularities at normal operating speeds without generating excessive vertical loads and stresses in the rails and track. And also vehicles shall be designed so that under all normal track and operating conditions they do not generate lateral forces which could jeopardize the structural integrity of the rails and track.

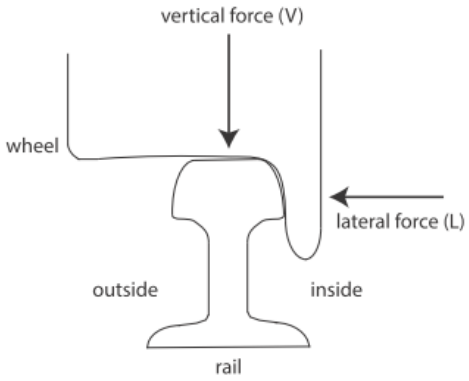

Figure 2.13 The lateral (L) and vertical (V) forces at a wheel-rail interface

2.3.5 Derailment coefficient

To determine the best criteria for predicting derailment of locomotive or rolling stock, there are many research has been carried out by the railway industry. In 1908 Nadal's, study determines derailment criteria, in the recent time work being done by Weinstock, Blader, Elkins and many others.

The estimate of the critical wheel L/V ratio was made by Nadal since 1908; Nadal imagined two point contacts between the wheel and rail at imminent derailment. Nadal further assumed that the first contact point, located on the thread, serves as an immediate point of rotation. He then equated the friction and normal forces at the second point, located on the wheel flange, with the lateral and vertical forces happening at the wheel rail interface, as shown in figure below. This resulted in his classic expression of wheel L/V ratio:

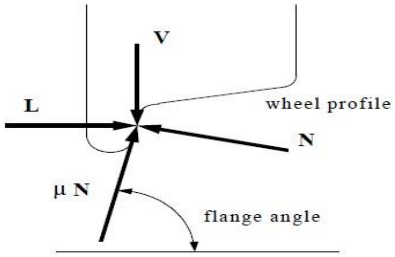

Figure2.14 Forces at wheel/rail interface

$$\frac{L}{V} = \frac{tan\delta - \mu}{1 + \mu tan\delta} \qquad (2.14)$$

Where, δ- is the flange angle and μ - is the coefficient of friction at the wheel/ rail contact point.

Nadal for his work use a flange angle of 65° and a coefficient of friction0.5, which resulted in critical $\frac{L}{V}$ ratio of 0.79. Consequently, it is suggested a limit of 0.80 for single wheel $\frac{L}{V}$ ratios. [14]

Conventionally limitation value of derailment coefficient is 1.2 (For an **70**˚ contact angle, and friction coe.of 0.35, L/V is calculated 1.22, normal applied), 0.9-1.2 (EN14363) 0.8 (such as specification for metro in China, UIC518).

2.3.6 Attack angle

As the wheel set negotiated on a shallow curve lateral slip will occur, this condition is described by [14] Based on the assumption that the center axle is aligned radially to the curve, at that time the outside axles sit slightly off-radial and have an angle of attack with the rail. This makes them forward velocities does not be tangential to the curve, on the contrary into and away from the outside rail for the leading and trailing axles, individually. As a result, the wheels have a tendency to roll to some extent laterally rather than directly following the curve's path. For the reason that the axle is constrained to move along the track, this lateral tendency is compensated for through lateral wheel slip. Wheel slip in whatever way, causes energy dissipation through frictional forces and brings inefficiency in the curving of the bogie.

Besides to the $\frac{L}{V}$ ratios, an additional factor that is important to evaluate the derailment is the angle of attack. For the same $\frac{L}{V}$ ratios, the wheel with a larger angle of attack has more possibility of derailment. Compared to a straight (none steering) truck, a steerable truck has an ability to negotiate a curve, with minimum angle of attack at the wheel/rail interface. The angle of attack is defined as the angle between a line perpendicular to the axle and center line of the track as shown below. [14]

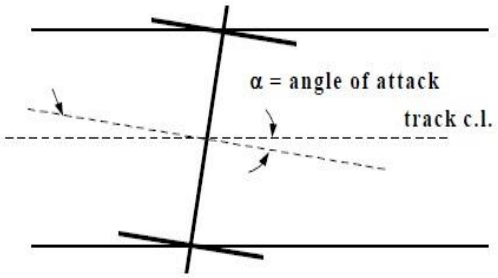

Figure 2.15 Angle of attack at wheel/rail interface

3. MODELING AND SIMULATION

3.1 Flexible wheelset modeling using FEMBS

FEMBS is an interface program between finite element (FE) analysis codes and SIMPACK. In finite element analysis (FEA) the motion of complex flexible structures is described by a large number of nodal co–ordinates, whereas SIMPACK codes use a nonlinear representation of rigid body motion, which is superimposed by small deformations. In SIMPACK elastic body deformation is described by a modal representation with a comparatively few number of modal co–ordinates. Finite element codes are appropriate tools for strain and stress analysis of flexible structures. However, the simulation of dynamic load cases is very time consuming, because of the high number of degrees of freedom. Thus, finite element analysis is appropriate to obtain detailed information about a component of a vehicle system for a few number of load cases. In contrast, many nonlinear mechanical systems, consisting of rigid bodies, control, and nonlinear components, are efficiently analysed by means of multibody system codes. This allows the dynamic behavior to be calculated for a number of different types of excitation. However, for lightweight components, elastic body deformation cannot be neglected, and in order to keep the numerical effort small, a reduced representation of elastic body deformation has to be established for SIMPACK [28].

Inputs for modeling wheelset:

- Advanced wheel profile shape: UIC-S1002
- Standard gauge :1435mm
- Diameter of the axle: 180mm
- Wheel diameter: 600mm
- Axle load: ≤11（1+3%）
- Conventionally about 70% used high strength steel grade 30 NiCrMoV12 steel properties are used to rail vehicle wheelset axle to get better performance in terms of weight and dimension. The success of 30 NiCrMoV12 steel of high strength was a consequence of its relevant mechanical characteristics, enabling the reduction of unsuspended masses and axle dimensions [26].
  - Young's Modulus (E) =180GPa
  - Poisson's Ratio = 0.3

- Density = 8900Kg/mm3
- Yield Strength = 490MPa
- Allowable load calculation :analytical calculation of Rail wheel axle to design the rail wheel axle firstly the diameter should bear the applied stress at a safe range. Taking the maximum vehicle load (i.e. overload) case and hence, 63.02tonnes of mass will be divided to the axles of the two bogies and hence to the eight wheels of the two bogies [21].

$$\text{Axle load} = \frac{\text{Vehicle weight+Cargo or passanger load}}{\text{Number of axle}} \qquad (3.1)$$

Since there are two bogies with four axles and eight wheels, axle load will be;

$$\frac{63{,}020kg * 9.81\,{}^{m}/_{s^2}}{4} = 154.56kN$$

Therefore, 154.56kN of weight will be divided to each of the two wheels of the four axles. In other words **77.28kN of weight will be carried by each wheel.** The wheels are assumed to be rigid and their nominal rolling circles are always perpendicular to the deformed wheelset axle at their interference fit surfaces.

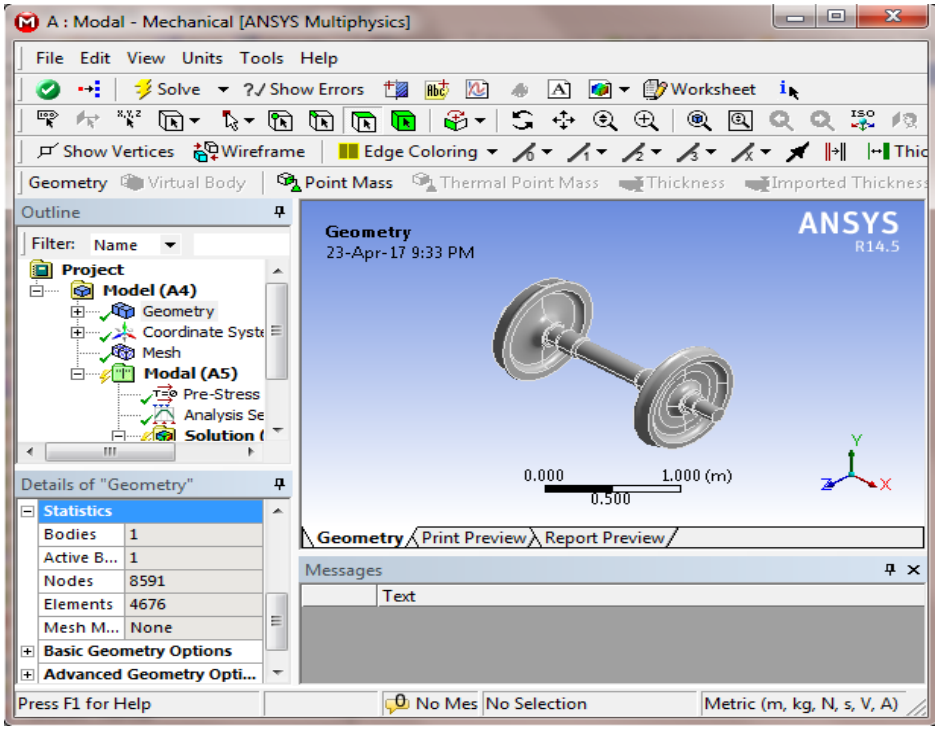

Figure 3.1 Wheelset model with constraints set on

The meshed model of the Rail wheel axle component is shown in the below figure.

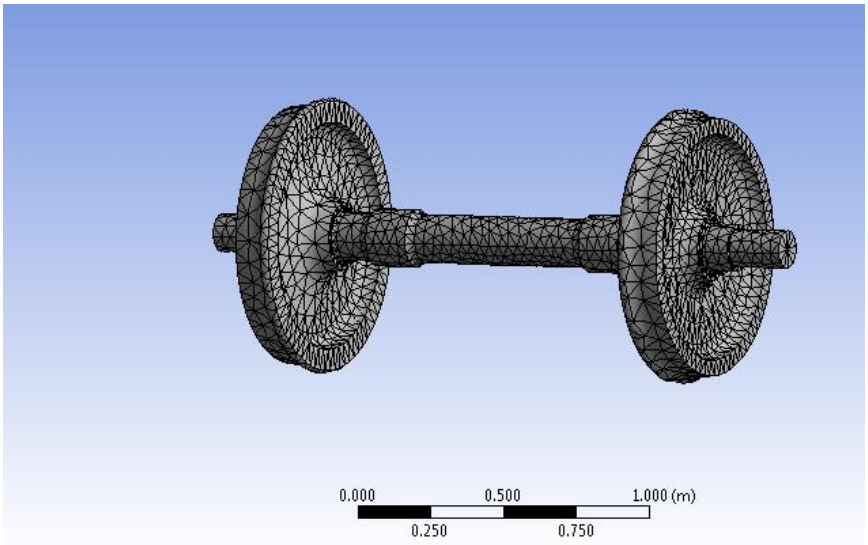

Figure 3.2 Fine meshed flexible wheelset model

The wheelset component fixed on each wheels is finely meshed with a total of 4676elements and 8591 nodes are created. Thus, the FE structure has 8589 x 3 = 25765DOFs. The motion of a flexible body of the MBS is subdivided into a large overall rigid body motion and small deformations represented by two modal co–ordinates (first and second bending).

Based on the modal synthesis method, these mode values of the wheelset are used to solve the motion equations of the flexible wheelset modeled as an Euler-Bernoulli beam. For every natural frequency there is a corresponding vibration mode shape. Most mode shapes can generally be described as being an axial mode, torsion mode, bending mode, or general modes. A crude mesh will give accurate frequency values. Modal analysis was carried out on Rail wheelset to determine the natural frequencies and mode shapes of a structure in the frequency range of 0 -1000 Hz [10].

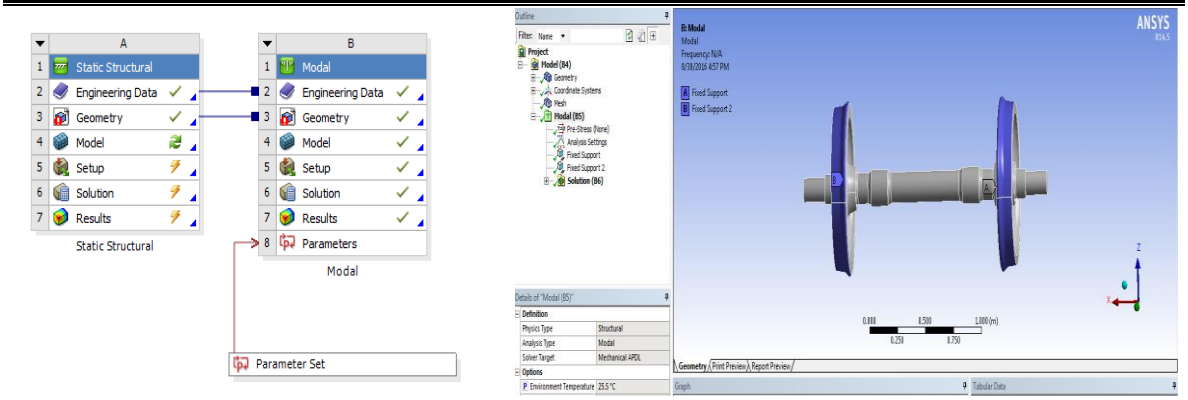

Figure 3.3 Task bars showing modal analysis done for wheelset

The commonly used simulation package, SIMPACK, was used to develop a wheelset model .The parameters of the SIMPACK model was used to generate wheel-rail forces and accelerations at the wheelset. These accelerations will be as the input conditions for the inverse mathematical model. In order to make the SIMPACK model replace a practical field test, the model developed with SIMPACK needs to be a very refined model.

Technical Specifications used as input [21]:

- **Rail profile** is UIC 60
- **Wheel profile:** UIC-S1002
- **Track gauge:** 1435m
- **Cant angle,** θ=1/40 =0.05 is used (Tee rails are generally installed at 1:40 cant in both tangent and curved track [19].) $\theta = \tan^{-1} {}^{1}/_{40} = 1.43^{0}$
- **Curve radius:** 50 meter **with length :** 93.48m (minimum curve radius located the way stadium to saris) [Appendix III]
- **Maximum allowable vehicle speed** on 50m curve is calculated using equation (2.13)

$$V_{max,on\ eleveted\ curve} = \sqrt{\frac{Rg[h\sin\theta + l\cos\theta]}{h\cos\theta - l\sin\theta}}$$

$$V_{max,on\ eleveted\ curve} = \sqrt{\frac{50*9.81[2.04\sin 1.43 + 0.75\cos 1.43]}{2.04\cos 1.43 - 0.75\sin 1.43}}\ m/s = 13.93 m/s$$

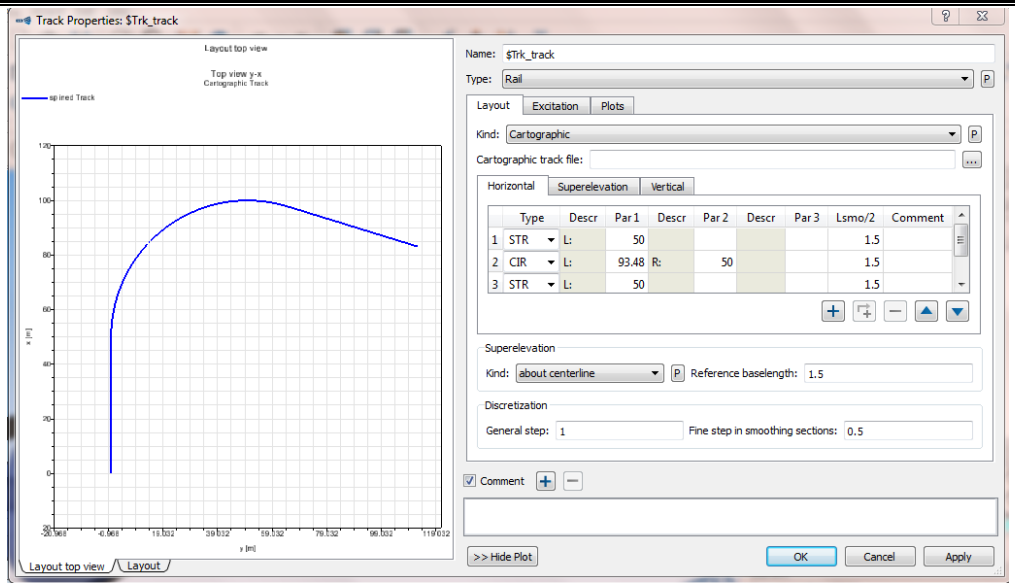

Figure 3.4 Task bar showing multi body model of track geometry which is similar for both flexible and rigid wheelset models

Elastic body representation in SIMPACK is often based on a set of eigenmodes which are calculated for the floating body in FEA. To describe the influence of loads within force elements, constraints, and joints on elastic body representation, it is frequently recommended to calculate so–called static modes. Static modes are obtained by applying static loads at attachment points, calculating the corresponding deformation by finite element analysis and using this static deformation as a mode shape for multibody system analysis in combination with eigenmodes. The FE output file(s), which contain these data, are read by FEMBS within the SIMPACK preprocessing module and a so–called FBI (Flexible Body Input) file is generated by FEMBS. This FBI file has a format that does not depend on the used FE program anymore. SIMPACK reads a so–called Standard Input Data (SID) file in order to implement a flexible body. This file is generated by FEMBS [28]. The following list gives an overview of FEM data, which FEMBS needs in order to create the SID file:

a) description of nodes with respect to a body fixed reference frame,

b) degrees of freedom of all nodes,

c) mass matrix corresponding to the DOFs defined in b),

d) stiffness matrix corresponding to the DOFs defined in b),

e) translational and rotational mode shapes for the modal representation (corresponding eigenmodes specified by natural frequencies and mode shapes),

f) geometric stiffness matrices and load vectors due to reference unit loads such as linear accelerations, angular accelerations, angular velocities, nodal forces and torques.

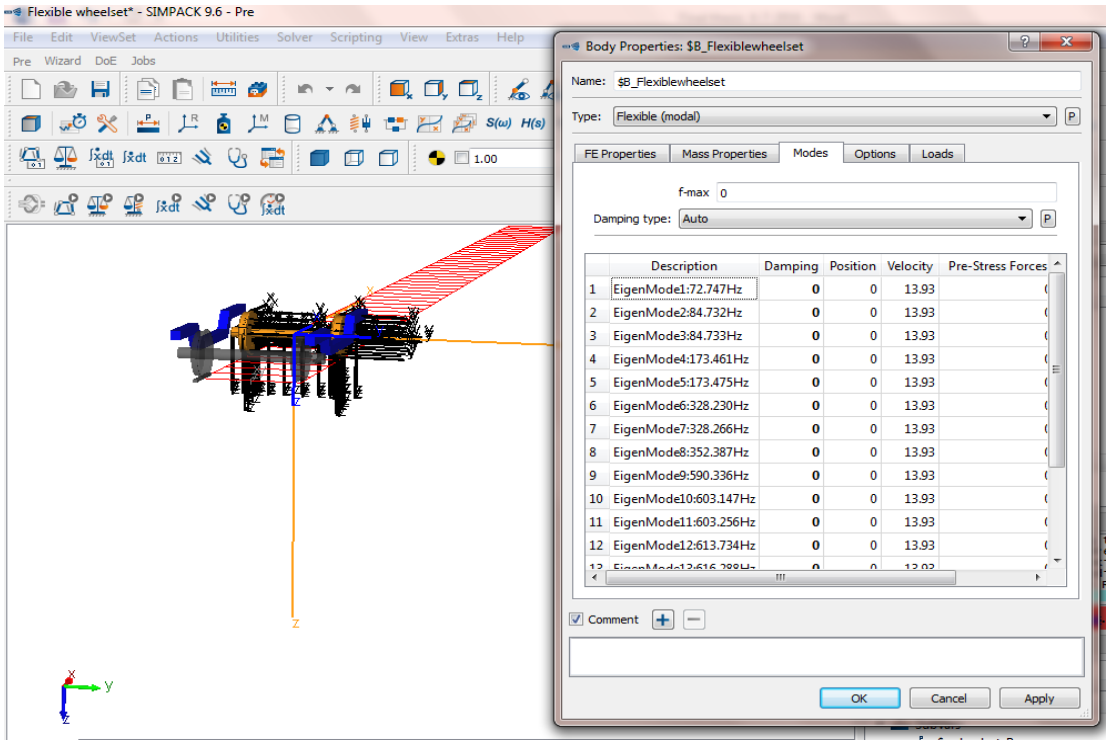

Figure 3.5 Task bars showing multi body model of flexible wheelset pairs on a bogie frame

3.2 Rigid wheelet modeling using SIMPACK

For a purpose of simulation result comparison, rigid wheelset model is developed directly using multi body simulation software SIMPACK in this section. As commonly used on rail vehicle design, two wheels rigidly connected by a common axle wheelset model with 6 degree of freedoms is modeled as rigid body as shown in figure 3.6 below.

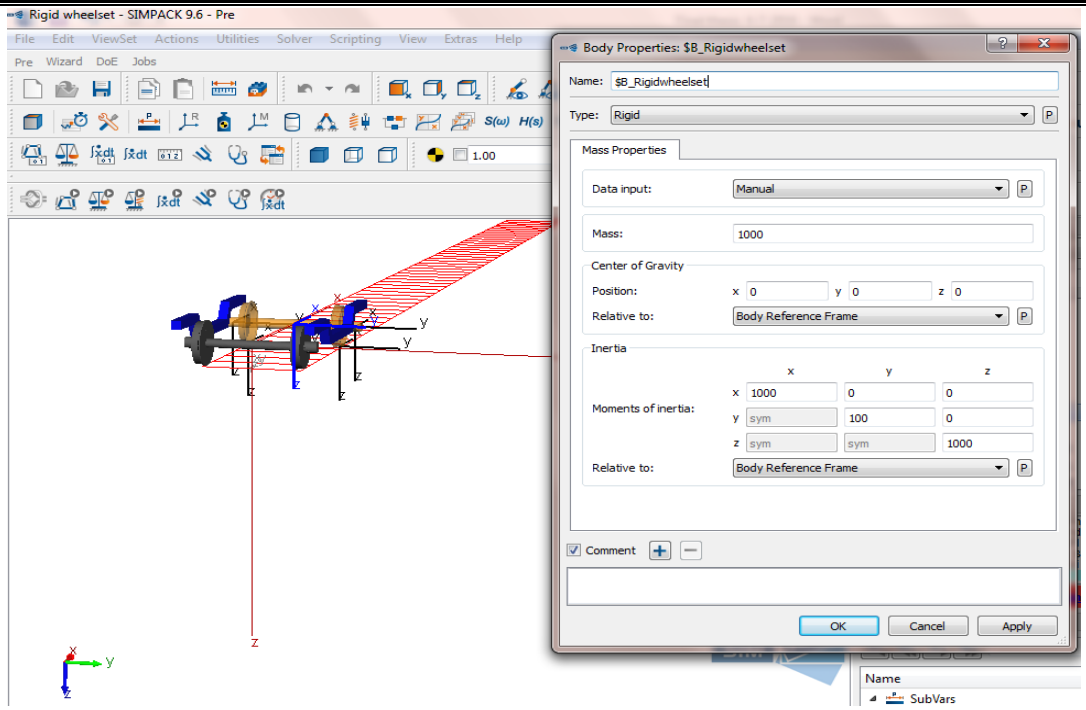

Figure 3.6 Task bars showing multi body model of rigid wheelset pairs on a bogie frame

3.3 Simulation results and discussion

3.3.1 Lateral displacement

In curve, a lateral displacement of wheelset is necessary in order to form a difference of rolling radius between outer and inner wheel, so that pure rolling on this curve possible. As shown in the figure 3.6 of the time domain results of the lateral deviation of flexible and rigid models of the wheelsets from the center of the track,

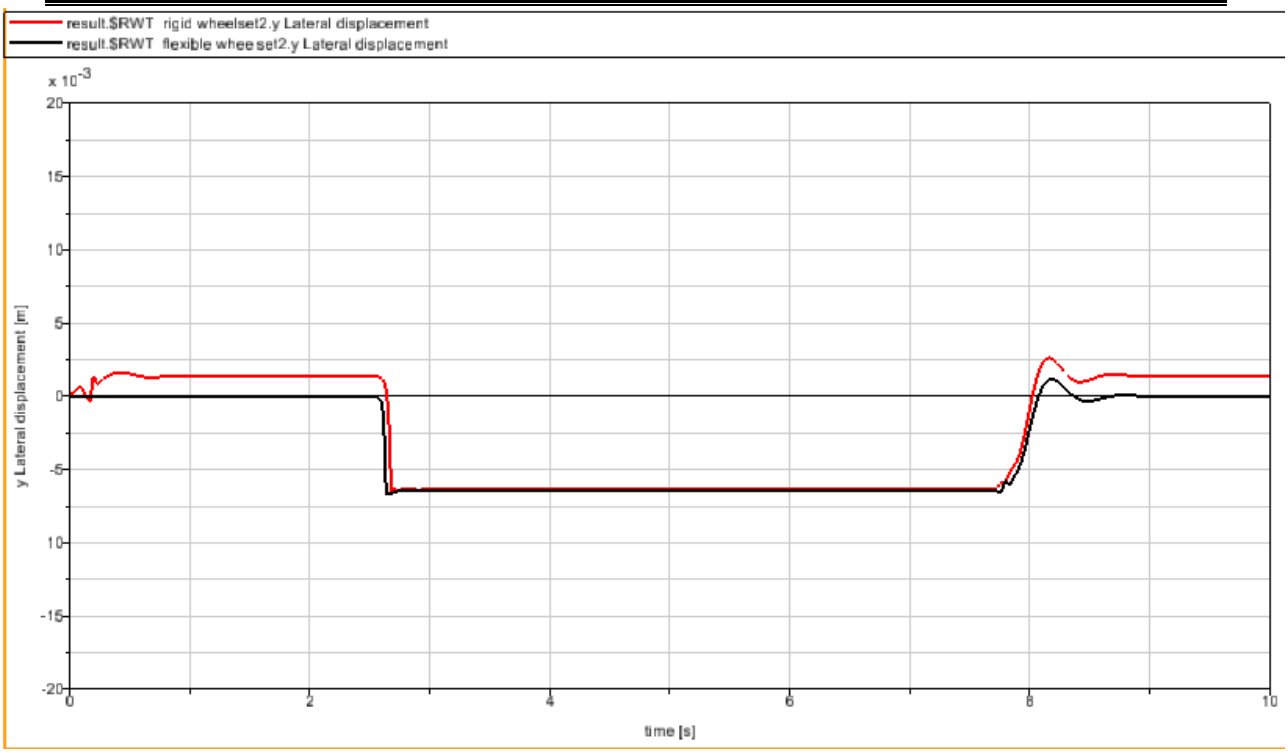

Figure 3.7 Time domain simulation result lateral displacement of flexible and rigid wheelsets

the characteristics curves for the lateral desplacement are almost equivalent. The peak value is about 7mm at the time of between around 2.7 ~ 7.7second. The limitation of wheel to rail (W/R) clearance is 7-10mm.

3.3.2 Lateral force

The wheel-rail contact force is affected by the position of the lateral contact points. In sharp curves, the wheel flange is on the inside, that the lateral force applied by the rail to the leading wheelset is applied to the outer wheel and will be combined with an enhanced vertical load, diminishing the risk of derailment. The wheel flanges will impact the rails, potentially causing damage to both the wheel and track, and in more serious cases causing sufficient lateral forces for the wheel to mount the rail, derailing the car.

Lateral forces of the flexible and rigid wheelsets acting on the rail are shown in the time domain simulation result figure 3.8.

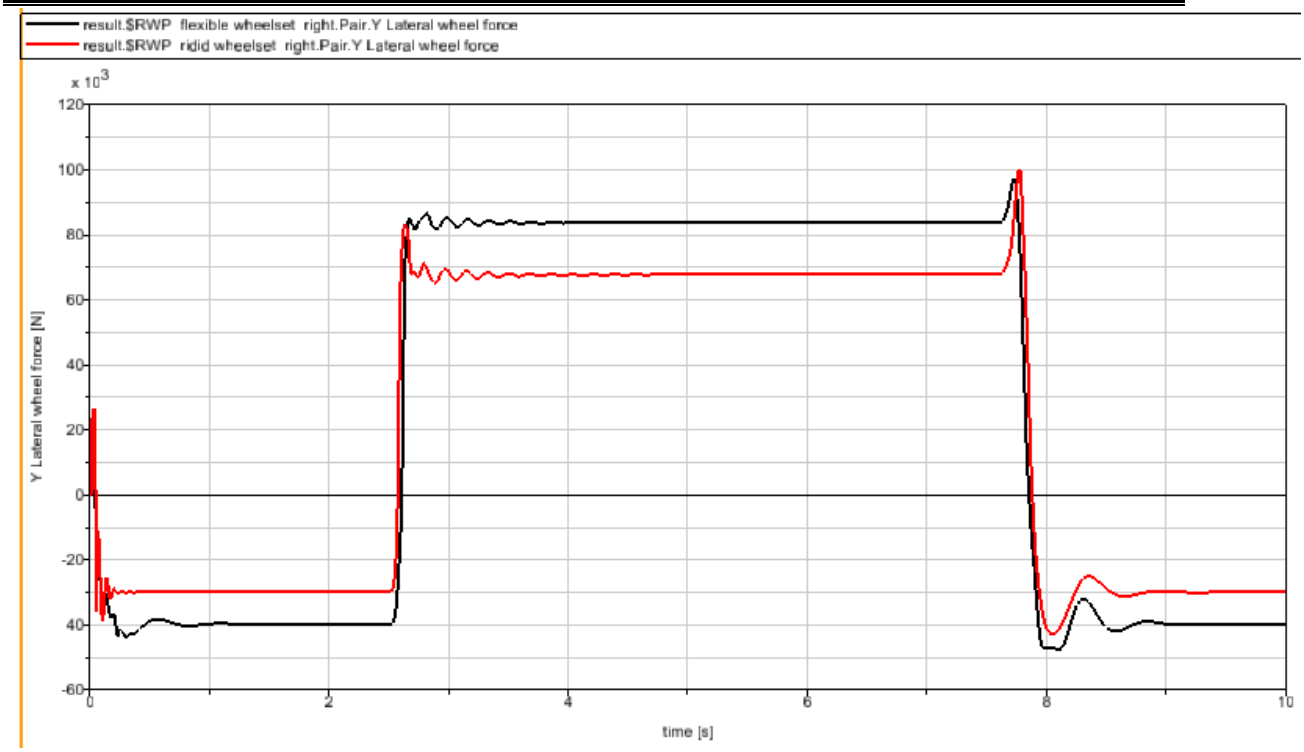

Figure 3. 8 Lateral wheel-rail contact forces of flexible and rigid wheelsets

The simulation result of SIMPACK software in figure 3.8 shows that about on 7.7second of the peak values lateral force of flexible and rigid wheelsets are 100KN and 93KN respectively. The simulation result verifies that the lateral force of the flexible wheelset is greater than the rigid wheelset by about 7KN. The maximum limit value of lateral force on track by wheelsetis 93 KN that is possible occurred while negotiating a sharp curve with a big cant deficiency.

3.3.3 Angle of attack

Attack angle is unavoidable, so rail -wheel pair interaction is always running with attack angle and flange contact. As the above figure indicates the angle of attack at wheel/rail interface during curve negotiation of flexible wheelset is greater than the rigid wheelset model after the half time of running time. In figure 3.9 is observed that,

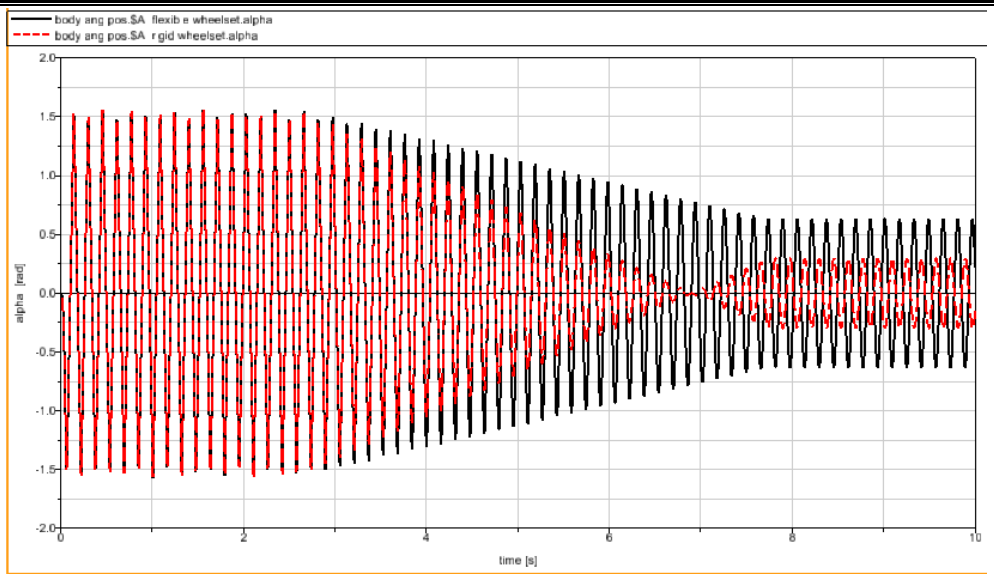

Figure 3. 9 Time domain simulation result for angle of attack of flexible and rigid wheelsets

after about 2.5 second the flexible wheelset's attack angle is higher with the rigid wheel. The positive and negative values on the graphs show that the wheelset is directed towards the inside and outside of the curve respectively, so that the positive value is advantageous.

3.3.4 Derailment coefficient

Limitation value of derailment coefficient1.2 (For an **70**˚ contact angle, and friction coefficient of 0.35, Y/Q is calculated 1.22, normal applied), 0.9-1.2 (EN14363) 0.8 (such as specification for metro in China, UIC518). As the simulation result of figure 3.10 indicates,

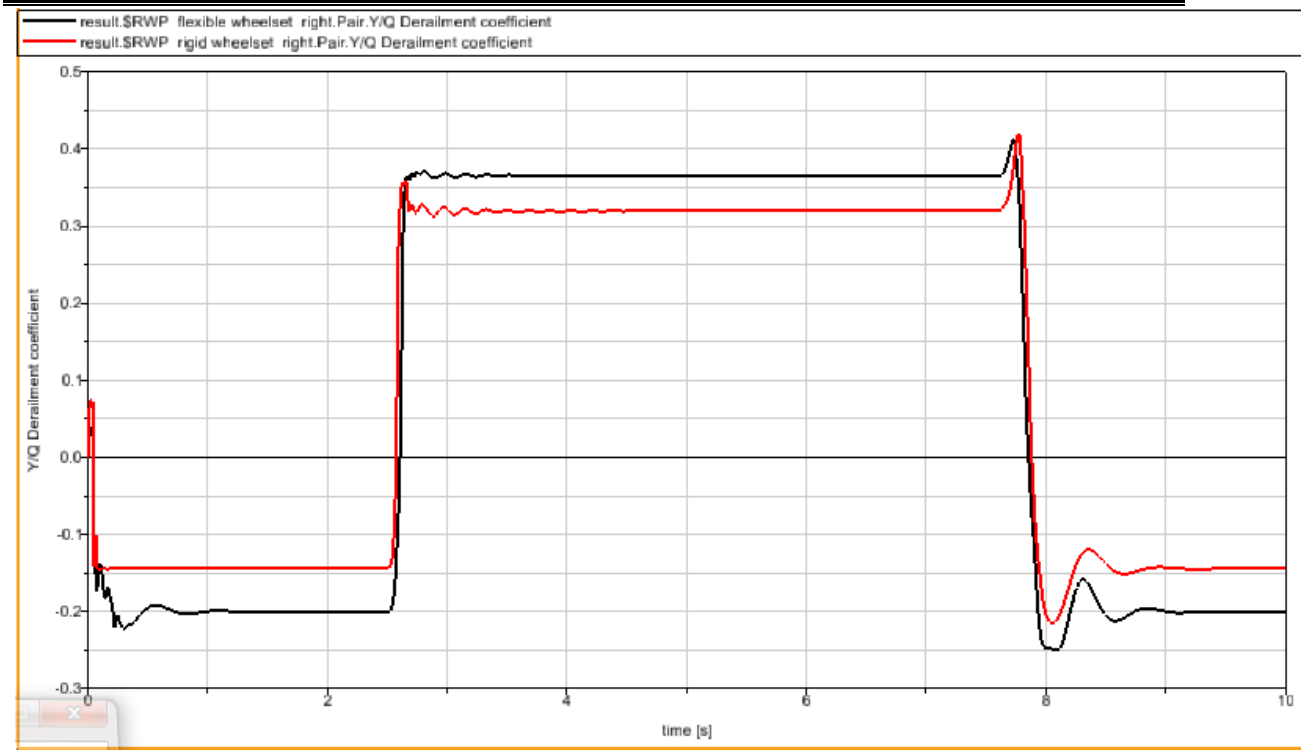

Figure 3. 10 Time domain simulation result of derailment coefficient of flexible and rigid wheelsets

derailment coefficient is lower for the rigid wheel when negotiating the curve.

3.3.5 Wear size

The wear of wheels and rails, especially the wheel flange wear and the rail side wear on curves, is a long-standing problem of railways. Severe wheel-rail dynamic interaction will induce serious wear of wheels and rails, especially in the case of curved tracks.

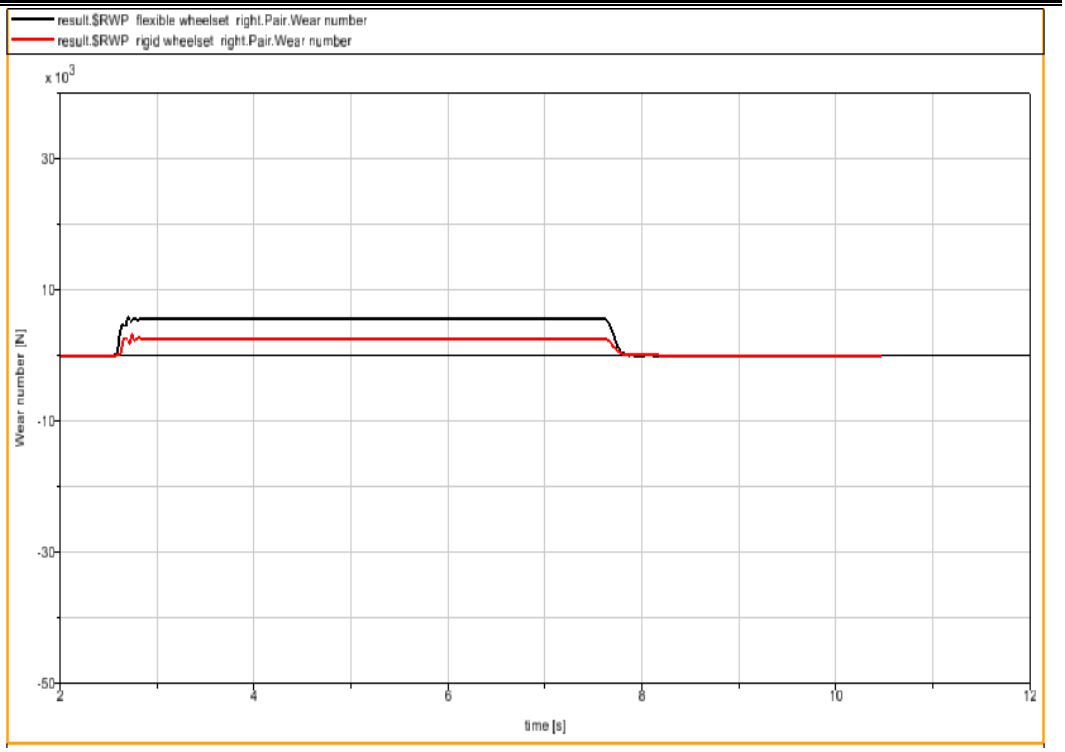

Figure 3.11 Time domain simulation result of wear size of flexible and rigid wheelsets

As the wheelset generates higher friction power specifically during curve negotiation due to higher lateral forces in which excessive wear occurs between wheel and rails. The wear graphs show that, as the vehicle moves over this curve, lower wear rate for the rigid wheelset.

4. CONCLUSION

The wheelset structural flexibility is the factor known to influence the vehicle-track interaction and contribute to higher frequency content of the wheel-rail forces. Proper representation of wheelset flexibility is important in analyzing wheel-rail contact behaviors and to predict wheel and rail fatigue damage. According to previous work in this field, the wheelset structural flexibility can also influence various aspects such as vehicle stability, wheel out-of roundness, wheel-rail corrugation and noise propagation.

In this thesis simulation of wheelset models that can evaluate the dynamic performance of both flexible and rigid wheels is presented. Simulated results showed that the average of the oscillation of the lateral contact force acting on the track by flexible wheelet model is larger than the rigid wheelset model. The angle of attack at wheel/rail interface during curve negotiation of flexible wheelset is also greater than the rigid wheelset model after the half of running time. As the wear result shows the wheelset generates higher friction power specifically during curve negotiation due to higher lateral forces in which excessive wear occurs between wheel and rails, that the flexible wheelset wear no. is larger average than the rigid wheelset. As a results of this thesis reveals, pertinent wheelset modelling with structural flexibility is necessary for proper investigation of different aspects of the vehicle-track dynamic interaction and in order to propose targeted changes on design.

Further work should assess the combined influence of the wheelset and track flexibilities on wheel rail forces at curve negotiation. Vehicle lateral stability should also be studied with respect to the flexibilities mentioned.

References

[1]. Kaiser I and Popp K: The Running Behaviour of an Elastic Wheelset, XXI ICTAM, Warsaw, 15-21 August 2004.

[2]. Kaiser I and Popp K: Interaction of Elastic Wheelsets and Elastic Rails: Modelling and Simulation. Proceedings of the 19th IAVSD Symposium on dynamics of vehicles on roads and on tracks, Vehicle System Dynamics Supplement, 44 (2006), pp. 932-939.

[3]. Andersson C and Abrahamsson T: Simulation of Interaction Between a train in general motion and a track. Department of Solid Mechanics, Chalmers University of Technology, Göteborg 2000.

[4]. Johansson A and Nielsen J: Out-of-Round Railway Wheels - A Literature Survey department of Solid Mechanics, Chalmers University of Technology, Göteborg 1998.

[5]. Morys B: Enlargement of Out-of-Round Wheel Profiles on High Speed Trains.Journal of Sound and Vibration (1999) 227(5), pp. 965-978.

[6]. Grassie S, Elkins J and Handal S: Rail Corrugation Mitigation in Transit. TransitCooperative Research Program, Research Results Digest, No 26, June 1998.

[7]. Matsumoto A, Sato Y, Tanimoto M and Qi K: Study on the Formation Mechanism of rail corrugation on Curved Track. Vehicle System Dynamics Supplement 25(1996), pp. 450 465.

[8]. Matsumoto A, Sato Y, Tanimoto M and Qi K: Wheel-Rail Contact Mechanics at Full scale on the Test Stand. Wear 191 (1996), pp. 101-106.

[9]. Tassilly E and Vincent N: A Linear Model for the Corrugation of Rails. Journal of sound and Vibration (1991), 150(1), pp. 25-45.

[10]. Meinders T: Modelling of a Railway Wheelset as a Rotating Elastic Multibody system. Machine Dynamic Problems, Vol. 20, 1998, pp. 209-219.

[11]. Hempelmann K, Ripke B and Dietz S: Modelling of Dynamic Interaction of Wheelsetand Track. Railway Gazette International, September 1992.

[12]. A. H. Wickens, Fundamentals of rail vehicle dynamics: guidance and stability. Lisse: Swets & Zeitlinger, 2003.

[13]. A.H. Wickens. History of railway vehicle dynamics. 2006 by Taylor & Francis Group, LLC

[14]. Michael DElorenzo Thesis faculty of Virginia Poltechnic Institute and state university NUCARS modeling of freight locomotive with steerable trucks may,20, 1997 page 16-17

[15]. Knothe, K., and Grassie, S.L., "Modeling of railway track and vehicle/track interaction at high frequencies", Vehicle System Dynamics 22 1993, pp. 209 – 262.

[16]. Simon Iwnicki, "Handbook of railway vehicle dynamics, United States of America", 2006.

[17]. Ing. Karel Zinke "The effect of axles´ flexibility to simulation´s results of the rolling stock ride"

[18]. A.B Perrlman and H.Weinstock, "Preliminary analysis of the effects of non-linear creep and flange contact forces on truck performance in curves" May 1975

[19]. Track guy consultants, Canonsburg, PAWilson, ihrig & associates, inc.Emeryville, CA"Track Design Handbook for Light Rail Transit" Second edition, 2012

[20]. Ing. Karel Zinke Vedoucí práce: doc. Ing. Josef Kolář CSc."The effect of axles´ flexibility to simulation´s results of the rolling stockride"

[21]. China Railway Group (CRECG) Project for Light Rail Project of Ethiopia, Technical Specifications of Vehicles, July 2013

[22]. Joanna Charlotte Moody,Bates College "Critical Speed Analysis of Railcars and Wheelsets on Curved and Straight Track"Spring 5-25-2014

[23]. World Trade Press Online. Guide to railcars. Available at http://worldtraderef.

com/WTR_site/Rail_Cars/Guide_to_Rail_Cars.asp.

[24]. Ken Harris and Jackie Tee. *IHS Jane's World Railways*. Janes Information Group, 54 edition, November 2012.

[25]. "UIC type A axle 20 t + high performance operation (overload) clarification "Joint Sector Support Group for ERA Task Force on wagon/axle maintenance Brussels 02, December 2009.

[26]. "High strength alloyed standard railway axle steel in compliance with European norms" Giampaolo Manchini and Alessandro Corbizi

[27]. "UIC 519 CODE" 1st edition, December 2004.

[28]. How to Use FEMBS within SIMPACK 8.5

Appendix I

Table 1. Common parameters of train model [19]

Wheelbase (power bogie)	1900 mm
Wheelbase (unpowered bogie)	1800 mm
Clear height of passenger compartment	≥1980 mm
Wheel diameter (new wheel)	≤660 mm
Wheel diameter (Max. wear)	≤600 mm
Side doors of passenger compartment	four pairs per side
Clear opening of passenger compartment door (width x height):	≥1300×1860 mm

Table 2. Rated passenger capacity of vehicle

Number of passengers (persons)	Seated	Standing	Total
Seats (AW_1)	65	0	65
Rated passenger capacity(AW_2) (standing: 6 persons/m^2)	65	189	254
Overload capacity (AW_3)(standing: 8 persons/m^2)	65	252	317

Table 3. Vehicle weight

Loads	Car body weight	Passenger weight	Total weight
Empty vehicle (t)	44	0	44
Rated passenger capacity (t)	44	15.24	59.24
Overload (t)	44	19.02	63.02
Axle load (t)	≤11（1+3%）t		

Appendix II

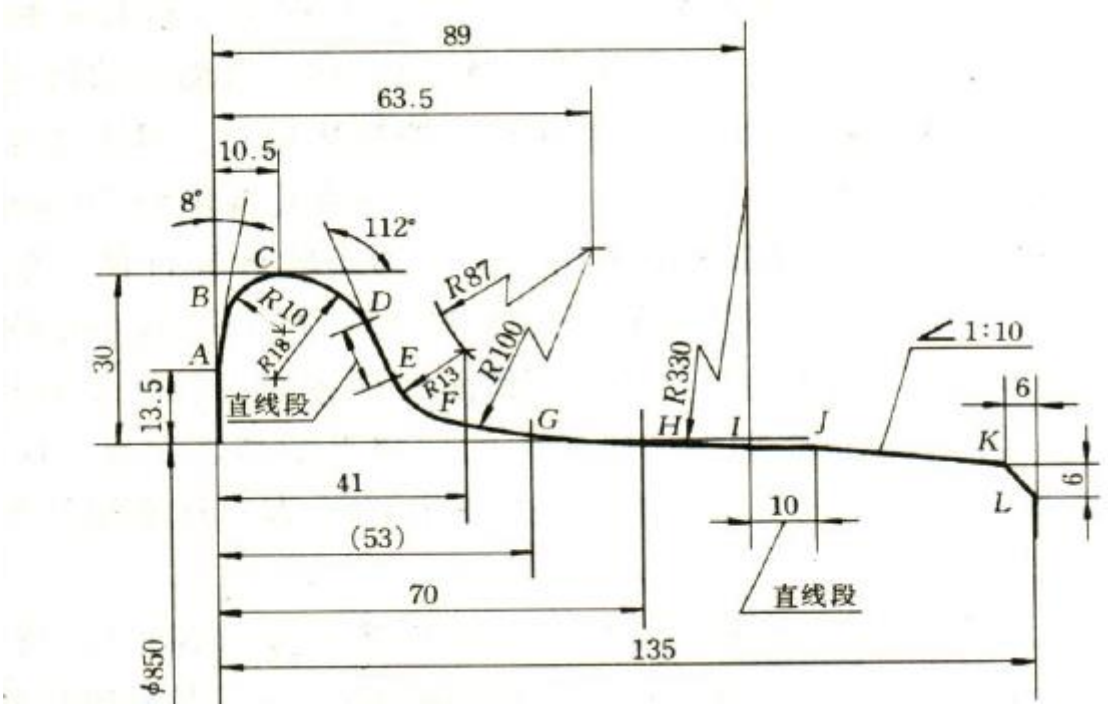

Figure I Worn type wheel profile (S1002)

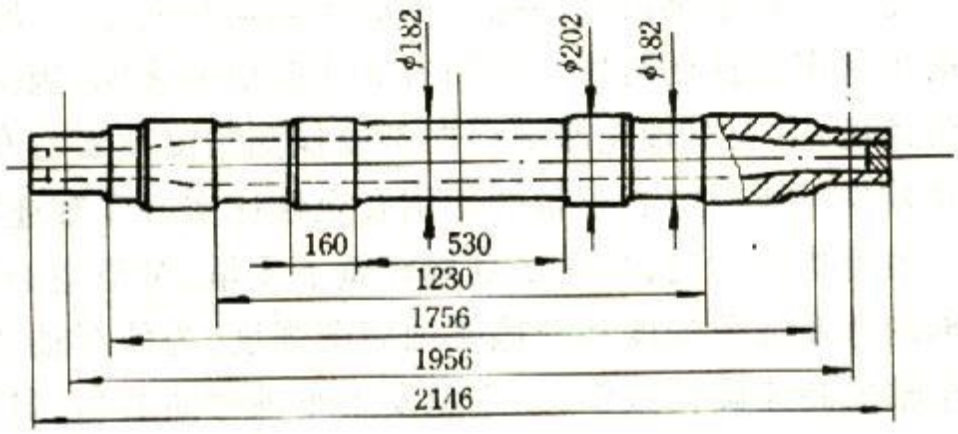

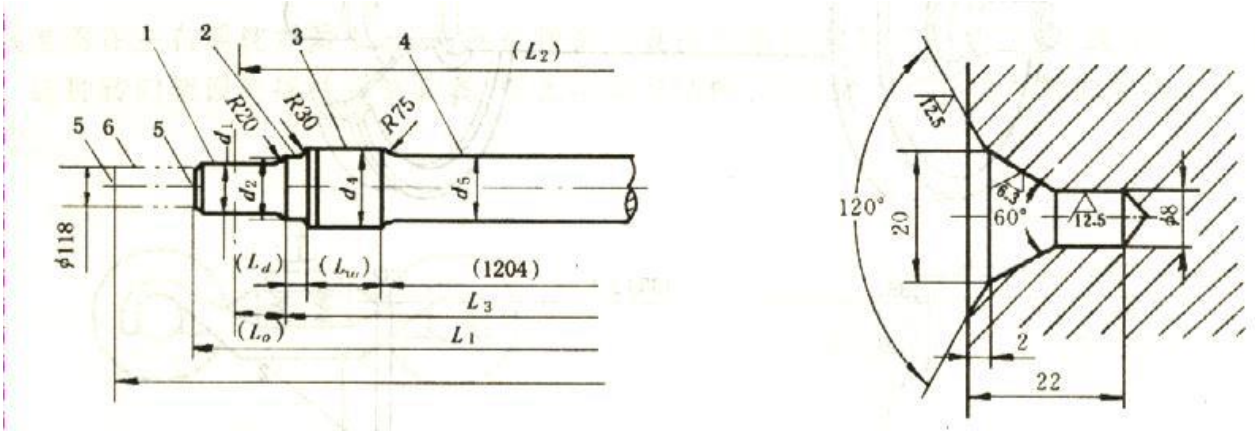

1.Axle journal, 2.dust guard seat, 3.wheel seat, 4. axle middle

Figure II Axle detail drawing

Figure III. AALRT track sub-layout drawing [21]